

Finite-Size Effects in Dynamics: Critical vs Coarsening Phenomena

Subir K. Das^{1,*}, Sutapa Roy¹, Suman Majumder¹ and Shaista Ahmad^{1,2}

¹*Theoretical Sciences Unit, Jawaharlal Nehru Centre for Advanced Scientific Research, Jakkur P.O, Bangalore 560064, India*

²*School of Physical Sciences, Jawaharlal Nehru University, New Delhi 110067, India*

(Dated: September 3, 2018)

Finite-size effects in systems with diverging characteristic lengthscale have been addressed via state-of-the-art Monte Carlo and molecular dynamics simulations of various models exhibiting solid-solid, liquid-liquid and vapor-liquid transitions. Our simulations, combined with the appropriate application of finite-size scaling theory, confirm various non-trivial singularities in equilibrium dynamic critical phenomena and non-equilibrium domain coarsening phenomena, as predicted by analytical theories. We convincingly demonstrate that the finite-size effects in the domain growth problems, with conserved order parameter dynamics, is weak and universal, irrespective of the transport mechanism. This result is strikingly different from the corresponding effects in critical dynamics. In critical phenomena, difference in finite-size effects between statics and dynamics is also discussed.

PACS numbers: 64.70.Ja

In computer simulations, finite size of the systems poses enormous difficulty in studying problems where characteristic length scales diverge [1, 2]. E.g., in equilibrium critical phenomena [3] the correlation length (ξ) diverges as

$$\xi \approx \xi_0 \epsilon^{-\nu}, \quad (1)$$

where $\epsilon = |T - T_c|/T_c$, T_c being a critical temperature. On the other hand, when a homogeneous system is quenched inside the miscibility gap, the phase separation progresses via divergence of average domain-size, $\ell(t)$, as a function of time (t) [3–6] as

$$\ell(t) \approx At^\alpha, \quad (2)$$

where the exponent α depends upon the transport mechanism. This difficulty can, of course, be overcome via application of finite-size scaling theory [1, 2, 7]. Nevertheless, it is of immense importance to learn the effects of finite system size, e.g., the study of nucleation and growth in nano-scopic systems, structure and dynamics in ultra-thin films, etc., are of great independent interest. Also, an appropriate knowledge of the size effects helps judicious choice of the system size for the direct understanding of the problem in the thermodynamic limit so that any unexpected deviation from a prediction is not inappropriately attributed to the deficiency in system size.

While in static critical phenomena such problems are well addressed, the situation appears challenging in dynamics. It is certainly of fundamental importance to make a comparative study of finite-size effects in statics and dynamics. However, there are only a few computational studies [8–12] of dynamic critical phenomena due to the fact that here, in addition to finite-size effects, the critical slowing down brings in another major hurdle. So finite-size effects are not appropriately probed and were thought to be same as in statics. On the other hand, despite a lot of simulation studies over several decades, the finite-size scaling theory in non-equilibrium domain coarsening problems found only rare application [13–15] and the finite-size effects in this type of problems remained a challenging issue.

In this letter, in addition to confirming results for various singular behaviors in critical and coarsening phenomena, we address the issue of finite-size effects in these two sets of problems under a very general framework. For the critical phenomena, we present results for both static and dynamic properties from Monte Carlo (MC) and molecular dynamics (MD) simulations of a liquid-liquid (LL) phase transition in a binary Lennard-Jones (LJ) system [11]. On the non-equilibrium front, results for kinetics of phase separation are presented for LL transition using the same LJ system, for vapor-liquid (VL) phase transition in a single component LJ model [16] as well as for a solid binary mixture (SS) using Ising model. An unified picture for the finite-size effects is obtained in this case despite different transport mechanisms leading to different values [3–5] of α in solids and fluids. Finally, contrasting observation between the finite-size effects in the non-equilibrium dynamics and the equilibrium critical dynamics is discussed. While these interesting results are expected to initiate further theoretical studies, the methods used here will be of significant importance in fluid dynamics, glass transition and other condensed matter systems.

For the binary ($A + B$) liquid, we consider a model (belonging to the 3–d Ising critical universality class, d being the space dimension) where particles at continuous positions \vec{r}_i and \vec{r}_j , in a periodic box of linear dimension L (in units of the LJ particle diameter), interact (for $r < r_c$) via

$$u(r = |\vec{r}_i - \vec{r}_j|) = U(r) - U(r_c) - (r - r_c) \frac{dU}{dr} \Big|_{r=r_c}, \quad (3)$$

where

$$U(r) = 4J_{\alpha\beta}[(d_{\alpha\beta}/r_{ij})^{12} - (d_{\alpha\beta}/r_{ij})^6]; \quad \alpha, \beta \in A, B \quad (4)$$

is the standard LJ potential with the pairwise interaction strength $J_{AA} = J_{BB} = 2J_{AB} = J$ and LJ diameter $d_{AA} = d_{BB} = d_{AB} = d_0$. The second term on the right hand side of Eq.(3) stands for a truncation and shifting of the potential at $r = r_c$ which we chose to be $2.5d_0$. Finally, the third term ensures that both the potential and the force are continuous all along.

We simulate this completely symmetric model at a high density $\rho = Nd_0^3/V = 1$ that exhibits a liquid-liquid transition at the critical parameters $k_B T_c \simeq 1.423J$ and $x_A = x_A^c = 1/2$ ($x_A = N_A/N$; $N = N_A + N_B$, N_α being the number of particles of species α). For the sake of convenience, in the rest of the paper we set k_B , J , d_0 as well as the equal mass (m) of the particles to unity which in turn sets the LJ time unit $t_0 = (md_0^2/J)^{1/2} = 1$. Phase behavior and static concentration susceptibility (χ) for this model were calculated from MC simulation in the semigrand canonical ensemble [7, 11] whereas the transport properties were obtained from relevant Green-Kubo relations [5, 17] by using outputs from MD simulations (for $T > T_c$) in microcanonical ensemble that perfectly preserves hydrodynamics. For the VL transition ($T_c \simeq 1$, $\rho_c \simeq 0.32$) [18], the same model with only one species of particles was used. To probe the hydrodynamic effects in the kinetics of fluid phase separation, both the LL and VL systems were studied via MD simulations in NVT ensemble by quenching a homogeneous system (of critical composition or density) below the respective critical temperatures. Here the temperature was controlled via Nosé-Hoover thermostat [19] that is known to preserve hydrodynamics well. Finally, for the SS case, spin- $\frac{1}{2}$ critical (50 : 50) Ising model with hamiltonian

$$H = -J \sum_{\langle ij \rangle} S_i S_j; S_i = \pm 1, J = 1, \quad (5)$$

was studied via Kawasaki-exchange MC [7] simulation, where exchange between two neighboring spins consisted a trial move that preserves composition of up (A) and down (B) spins (particles). This introduces a diffusive dynamics which is responsible for domain coarsening in solid mixtures. An MC step (MCS) consisted of L^d trial moves.

The primary quantity of interest in the non-equilibrium phenomena is the average domain size, $\ell(t)$, which, unless otherwise mentioned, was obtained from the first zero crossing of the two-point equal-time correlation function [6] $C(r, t)$ where r is the distance between two points. For phase ordering dynamics with conserved order-parameter, while $\alpha = 1/3$ for diffusive domain-coarsening (which is the only coarsening mechanism in binary solids) [4–6], for fluids [16, 20–22] hydrodynamic mechanism plays important role and there a diffusive growth is followed by a viscous hydrodynamic one with $\alpha = 1$ and then by an inertial hydrodynamic regime with $\alpha = 2/3$. On the other hand, for critical dynamics we present results for the bulk viscosity (ζ) (we observe similar size effects in other relevant transport properties as well, however, do not present those here for the sake of brevity). Note that, analogous to Eq. (1), the critical singularity of any thermodynamic or dynamic property, X , is quantified as

$$X \approx X_0 \epsilon^{-x} \quad (6)$$

where $x = 0.63$, 1.239 , and 1.82 for ξ , χ and ζ , respectively [3, 10, 12, 23–28], for 3-d Ising universality class.

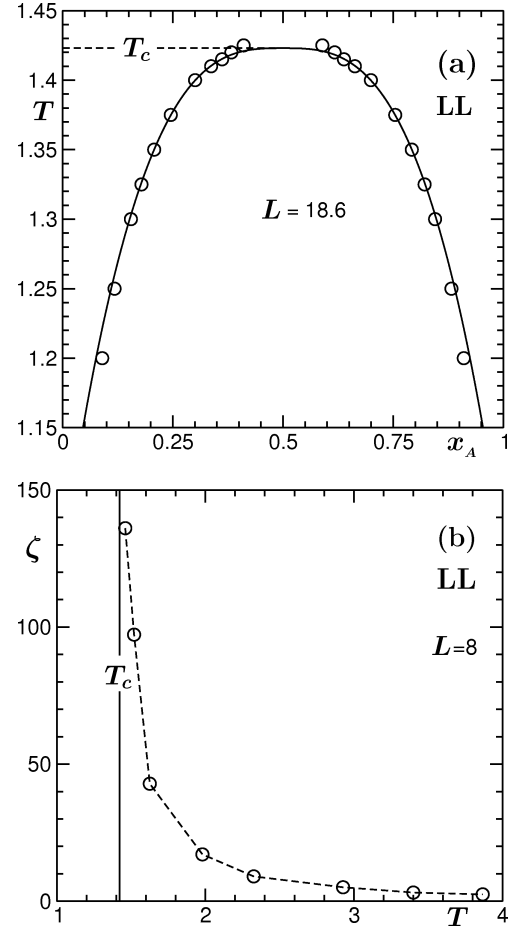


FIG. 1. (a) Phase behavior of the binary fluid model in temperature-concentration plane. The solid line there is a fit to the form $m = |\frac{1}{2} - x| \sim \epsilon^\beta$; $\beta = 0.325$ (Ising value), by choosing a region close to the critical point but unaffected by finite-size of the system. This provides $T_c = 1.423 \pm 0.002$. (b) Plot of bulk viscosity (ζ) vs temperature, for the same model, at the critical composition, for a system size $L = 8$. The vertical line corresponds to the critical temperature.

Unless otherwise mentioned, all results are presented in this space dimension.

For the sake of completeness, the phase diagram is shown in Fig.1(a), for a system of size $L = 18.6$. The continuous line there is a fit to the form $m = |\frac{1}{2} - x| \sim \epsilon^\beta$ by fixing β to its 3-d Ising value 0.325. Note that data only close to the critical point but unaffected by finite-size of the system were used. From this exercise, we obtain $T_c = 1.423 \pm 0.002$. In Fig.1(b) we present the simulation results for the bulk viscosity (ζ) as a function of temperature, for the binary LJ system, with $L = 8$. The data for ζ shows a sharp increase close to the critical point. While this signifies a strong critical divergence, a least-square fitting using the form (6) gives an exponent much smaller than 1.82 which could well be due to strong finite-size effects. Thus, an appropriate understanding of the result calls for the following finite-size scaling analysis. (Note that a general discussion of finite-size scaling analysis in this context is provided in Ref. [29]. However, for the sake of completeness we briefly discuss it here.) At the critical point, the singularity of X , as a function of

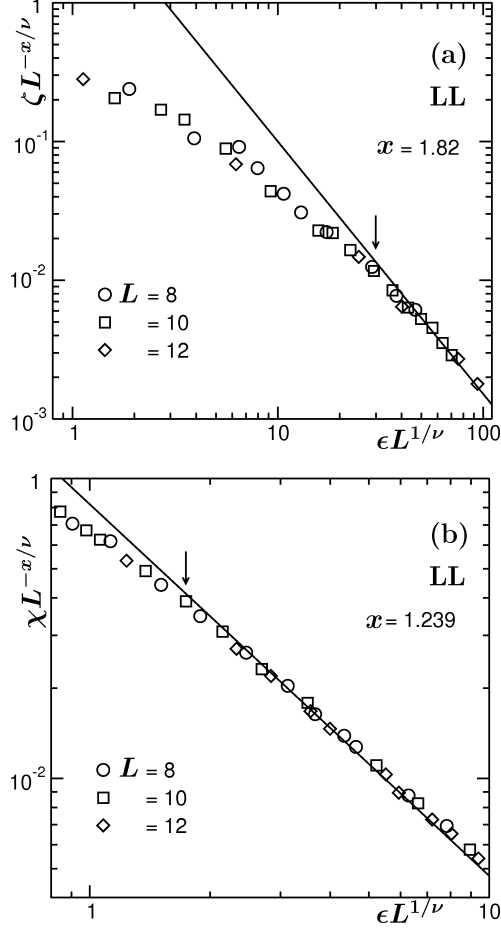


FIG. 2. (a) Finite-size scaling plot of ζ . Here $\zeta L^{-1.82/\nu}$ is plotted vs $\epsilon L^{1/\nu}$ by taking data from three different system sizes. The solid line there has a power-law behavior with exponent -1.82 . (b) Same as (a) but for χ by using $x = 1.239$.

the system size, is characterized as

$$X = A_0 L^{x/\nu}, \quad (7)$$

where $A_0 = X_0/(2\xi_0)^{x/\nu}$ and we have used the fact that $\xi = L/2$ at T_c . Away from T_c , one needs to introduce a scaling function $Y(y)$ to write

$$X = L^{x/\nu} Y(y), \quad (8)$$

where y is a function of the dimensionless variable L/ξ . While, $Y(y) = A_0$ at $T = T_c$, for the convenient choice $y = (L/\xi)^{1/\nu} (\propto \epsilon L^{1/\nu})$ and $T \gg T_c$ ($L \gg \xi$), one must have

$$Y(y) \sim y^{-x}, \quad (9)$$

so that Eq.(6) is recovered. Thus, when $XL^{-x/\nu}$ is plotted vs y , in addition to collapse of data coming from different system sizes, one should obtain a power-law behavior with the exponent $-x$, for $y \gg 0$. A deviation from this power-law, for smaller y , signals the onset of finite-size effects. In Fig.2 (a) and (b) this is demonstrated for ζ and χ , for the binary LJ model. Here we have fixed x at the respective values and used T_c as an adjustable parameter. The best collapse of data is obtained at $T_c \simeq 1.421$ which, of course, is consistent with the value quoted in

the caption of Fig.1. For large enough y , both the quantities are consistent with the expected critical behaviors represented by the solid lines. However, the striking difference between the onsets of significant finite-size effects (marked by arrows), quantified by the ratio $z_0 = \xi/L$, should be noted. It appears that $z_0 = \mathcal{O}(1)$ for χ and $= \mathcal{O}(10^{-1})$ for ζ .

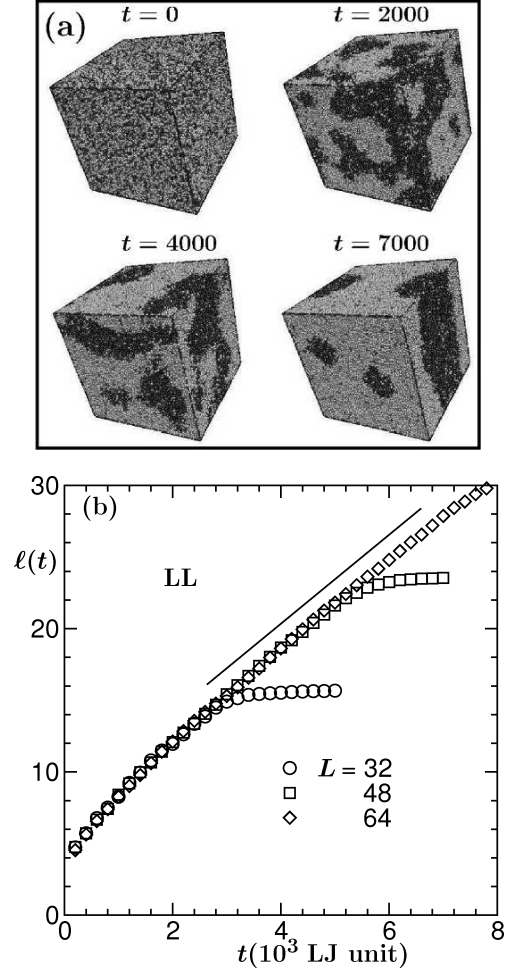


FIG. 3. (a) Evolution snapshots from four different times after quenching a homogeneously mixed 50 : 50 binary fluid, confined in a box of linear dimension $L = 64$, into the miscibility gap. (b) Plot of $\ell(t)$ as a function of t , for the model of (a). Results from 3 different system sizes are displayed. The solid straight line there corresponds to the linear viscous hydrodynamic growth. All results correspond to a temperature $T = 0.77T_c$.

We start the discussion of non-equilibrium phenomena from Fig.3(a) which demonstrates the formation and growth of A -rich and B -rich domains for $L = 64$ in a binary LJ fluid. Note that the thermal noise seen in the snapshots create difficulty in accurate estimation of the average domain size. This problem was avoided via following procedure. First we have mapped the continuum system into a L^3 lattice where a site occupied by an A -particle was assigned a spin value $+1$, otherwise -1 . Further, a majority spin rule, where the value of the spin at a site was replaced by the sign of the majority of the spins around it, was used to eliminate the noise. Note that for

LL, VL, as well as SS cases, the quantitative analysis was done by using the noise-free, so called “pure domain”, snapshots.

In Fig. 3(b) we show the plots of $\ell(t)$ (in units of LJ diameter) vs t , for three different system sizes, obtained after quenching a homogeneously mixed system to a temperature $T = 0.77T_c$. For $L = 64$, it is clearly seen that $\ell(t)$, beyond $t = 2 \times 10^3$, is growing quite linearly, consistent with an expected viscous hydrodynamic behavior. Even though, in this case the finite-size effects did not appear yet, for $L = 32$ and 48, the flat natures of the data towards the ends indicate that the equilibriums have been reached. It is interesting to notice that the results for the smaller systems follow the larger ones almost till the saturation limit. This is already suggestive of only weak size effects. Nevertheless, to correctly quantify it, we again take the help of finite-size scaling theory which, in addition, will provide further concrete information about the growth law.

In the present case, a finite-size scaling tool could be constructed by making the obvious identification of $1/t$ with ϵ and $\ell(t)$ with ξ . Then the relation equivalent to Eq. (8) is

$$\ell(t) = LY(y); \quad y = (L/\ell)^{1/\alpha} \propto L^{1/\alpha}/t. \quad (10)$$

Thus, when $\ell(t)L^{-1}$ is plotted vs y , for large y , a power-law behavior with an exponent $-\alpha$ should be obtained. For the sake of convenience, we demonstrate this first for the 2-d Ising model, quenched to the temperature $T = 0.6T_c$.

In Fig. 4(a), we show the direct plots of $\ell(t)$ (in units of lattice constant) vs t , for two different system sizes. In Fig. 4(b), we show a trial plot for the scaling behavior contained in Eq. (10) where, of course, we have correctly substituted L by the corresponding maximum domain length [see Fig. 4(a)], ℓ_{\max} , that represents the equilibrium limit. We have fixed $\alpha = 1/3$, as expected for diffusive domain growth in Kawasaki-exchange Ising model. Here, very poor quality of data collapse for large values of y is due to the fact that the systems do not enter the scaling regime immediately. In fact, after the quench the system requires a while to become unstable to fluctuations. Of course, this non-overlapping behavior will not be seen if one has data over many decades in time for a significantly large system. But this will be prominent for small systems. Thus, for a correct analysis, one needs to subtract a time t_0 from t (and corresponding length ℓ_0 from ℓ_{\max} as well as $\ell(t)$) to work with only the scaling part. Note that ℓ_0 is independent of time and is analogous to a weakly temperature dependent background contribution in critical phenomena. The correct value of t_0 (and so ℓ_0) must correspond to the optimum data collapse. This is illustrated in the Fig. 4(c) where excellent collapse is obtained for $t_0 = 20$. The solid line there has the form $y^{-\alpha}$ ($\alpha = 1/3$) with which, for $y \gg 0$, the simulation results are perfectly consistent. The point of deviation of the data from this solid line provides us with the information about the onset of finite-size effects at $\ell(t) \simeq 0.77\ell_{\max}$ which is informative of much weaker size effects compared to previous understanding. This now

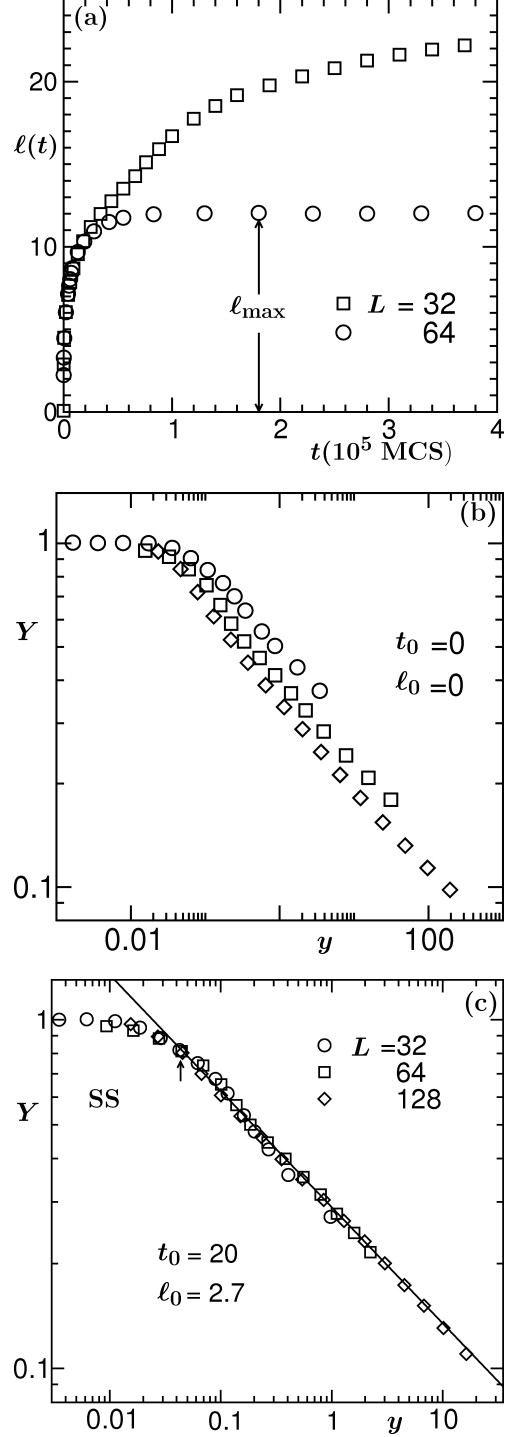


FIG. 4. (a) Plot of length scale $\ell(t)$ as a function of t , for 2-d Ising model, for two different system sizes as shown in the figure. (b) Finite-size scaling plot of $\ell(t)$, in accordance with Eq. (10) using 3 different system sizes with t_0 set to zero. (c) Same as (b) but t_0 (thus ℓ_0) was varied to obtain the optimum data collapse.

needs to be seen if this small finite-size effect is characteristic of only the simple Ising model or of more general validity. To investigate this, in the following we look back at the domain coarsening in fluids.

In Fig. 5 (a), we present the scaling plot of $\ell(t)$ for the binary LJ system of Fig. 3. As discussed, in fluid

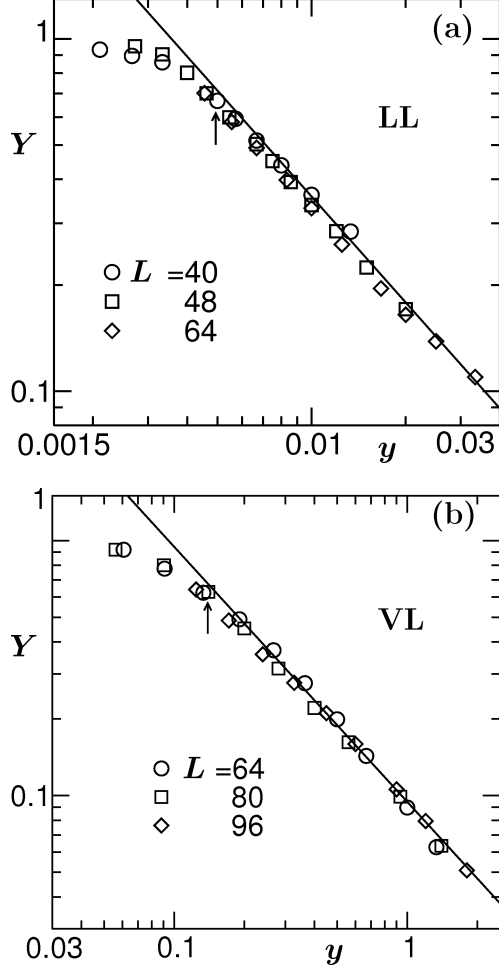


FIG. 5. Finite-size scaling plots of length scale data for the (a) binary LJ model and (b) single component LJ model. In (b), $\ell(t)$ was obtained from the first moment of the domain-size distribution function.

phase separation a diffusive domain growth is followed by a linear viscous growth and further by an inertial regime with an exponent $\alpha = 2/3$. Due to the obvious difficulty in dealing with significantly large system size for a long time, we are unable to observe the inertial growth. On the other hand, a gradual crossover to the linear regime from very early time does not allow us to observe a pure diffusive domain growth. Thus the focus in this exercise is to obtain a concrete answer for the linear behavior. On this occasion, a perfect data collapse could be obtained when the correct length (ℓ_c) and time (t_c), corresponding to crossover from diffusive to viscous regime, are subtracted. In Fig. 5 (a), the best collapse is obtained (by fixing $\alpha = 1$) for $t_c = 2 \times 10^3$ ($\ell_c \simeq 12$) which could also be appreciated from Fig. 3. The consistency of the master curve with the solid line (y^{-1}) provides further confirmation about the linear behavior. A deviation from this solid line occurs at $\ell(t) \simeq 0.8\ell_{\max}$ which is very similar to the Ising model (SS) scenario. In Fig. 5 (b), analogous exercise is demonstrated for the VL transition in a single component LJ fluid, for which we obtain $t_c = 50$. Here also, the presence of a linear viscous hydrodynamic growth is confirmed and we quantify the appearance of

finite-size effects at $\ell(t) \simeq 0.78\ell_{\max}$. Needless to say, the scaling would have failed if we were able to reach the inertial hydrodynamic regime by running a much bigger system for significantly longer period of time.

In summary, we have presented comprehensive results for the structure and dynamics from the state-of-the-art computer simulations of models exhibiting various phase transitions. It is demonstrated that the finite-size effects in equilibrium critical dynamics is much stronger compared to thermodynamics. Even though we believe that the finite-size effects in critical dynamics should be universal, as in the static case, this needs to be checked. On the other hand, the results for the non-equilibrium coarsening phenomena is suggestive of only weak size effects which is in sharp contrast with traditional understanding. Also, this non-equilibrium size effect appears to be universal for coarsening in solid-solid, liquid-liquid and vapor-liquid phase transitions which we have quantified to be appearing at $\ell(t) \simeq (0.8 \pm 0.1)\ell_{\max}$. This result should be compared with the work of Ref. [13] where it was pointed out that the finite-size effect is strong. Note that in the latter work, only an off-critical composition was used and a final conclusion, for the appearance of finite-size effects, was drawn as a fraction of the system size L . Thus, the problem of off-critical composition may be revisited for more accurate conclusions in terms of ℓ_{\max} . Also, it would be interesting to test our claim about the universally weak finite-size effects via further studies at different quench depth.

Further, via appropriate applications of finite-size scaling theory, we show that our results are consistent with the expected theoretical predictions related to the divergence of relevant quantities, both for equilibrium and non-equilibrium dynamics, in the thermodynamic limit.

The authors acknowledge grant No. SR/S2/RJN-13/2009 of the Department of Science and Technology, India, for financial support. SR and SM acknowledge Council of Scientific and Industrial Research and SA acknowledges University Grants Commission for financial support. SA is grateful to JNCASR for hospitality during her research visits.

* das@jncasr.ac.in

-
- [1] FISHER M.E. in *Critical Phenomena*, edited by GREEN M.S., (Academic Press, London, 1971) p.1.
 - [2] FISHER M.E. and BARBER M.N., *Phys. Rev. Lett.* **28**, 1516 (1972).
 - [3] ONUKI A., *Phase Transition Dynamics* (Cambridge University Press, UK, 2002).
 - [4] BINDER K., in *Phase Transformation of Materials* (Weinheim, VCH, 1991), Vol. 5, p. 405.
 - [5] BRAY A.J., *Adv. Phys.* **51**, (2002) 481.
 - [6] *Kinetics of Phase Transitions*, edited by PURI S. and WADHAWAN V. (CRC Press, Boca Raton, 2009).
 - [7] LANDAU D.P. and BINDER K., *A Guide to Monte Carlo Simulations in Statistical Physics*, 3rd Edition (Cambridge University Press, Cambridge, 2009).
 - [8] JAGANNATHAN K. and YETHIRAJ A., *Phys. Rev.*

- Lett.* **93**, (2004) 015701.
- [9] CHEN A., CHIMOWITZ E.H., DE S. and SHAPIR Y., *Phys. Rev. Lett.* **95**, (2005) 255701.
 - [10] DAS S.K., FISHER M.E., SENGERS J.V., HORBACH J. and BINDER K., *Phys. Rev. Lett.* **97**, (2006) 025702.
 - [11] DAS S.K., HORBACH J., BINDER K., FISHER M.E. and SENGERS J.V., *J. Chem. Phys.* **125**, (2006) 024506.
 - [12] ROY S. and DAS S.K., *EPL* **94**, (2011) 36001.
 - [13] HEERMANN D. W., YIXUE L. and BINDER. K., *Physica A* **230**, (1996) 132.
 - [14] MAJUMDER S. and DAS S.K., *Phys. Rev. E* **81**, (2010) 050102.
 - [15] MAJUMDER S. and DAS S.K., *Phys. Rev. E* **84**, (2011) 021110.
 - [16] MAJUMDER S. and DAS S.K., *EPL* **95**, (2011) 46002.
 - [17] HANSER J.-P. and McDONALD I.R., *Theory of Simple Liquids* (Academic Press, London, 2008).
 - [18] For a discussion on these values see [16] and Ref. [41] therein.
 - [19] FRENKEL D. and SMIT B., *Understanding Molecular Simulations: From Algorithm to Applications* (Academic Press, San Diego, 2002).
 - [20] SIGGIA E.D., *Phys. Rev. A* **20**, (1979) 595.
 - [21] FURUKAWA H., *Phys. Rev. A* **31**, (1985) 1103; *ibid* **36**, (1987) 2288.
 - [22] AHMAD S., DAS S.K. and PURI S., *Phys. Rev. E* **82**, (2010) 040107.
 - [23] ONUKI A., *Phys. Rev. E* **55**, (1997) 403.
 - [24] OLCHOWY G.A. and SENGERS J.V., *Phys. Rev. Lett.* **61**, (1988) 15.
 - [25] LUETTNER-STRATHMANN J., SENGERS J.V. and OLCHOWY G.A., *J. Chem. Phys.* **103**, (1995) 7482.
 - [26] HAO H., FERRELL R.A. and BHATTACHARJEE J.K., *Phys. Rev. E* **71**, (2005) 021201.
 - [27] BHATTACHARJEE J.K., IWANOWSKI I. and KAATZE U., *J. Chem. Phys.* **131**, (2009) 174502.
 - [28] BHATTACHARJEE J.K., KAATZE U. and MIZZAEV S., *Rep. Progr. Phys.* **73**, (2010) 066601.
 - [29] CHIMOWITZ E.H., *Introduction to Critical Phenomena in Fluids* (Oxford University Press, 2005).